C. R. Chimie 22 (2019) 686–694

Contents lists available at ScienceDirect

Comptes Rendus Chimie

www.sciencedirect.com

Full paper / Mémoire

Novel R_3M (M = Si, Ge) substituted furan and thiophene-derived aldimines: Synthesis, electrochemistry, and biological activity

Nouvelles aldimines dérivées du furanne et du thiophène substituées par R_3M (M = Si, Ge) : Synthèse, électrochimie et activité biologique

Jana Spura [a], Amel Farhati [c], Vitalijs Romanovs [a, b, *], Artyom Borodulin [a], Sergejs Belakovs [a], Juris Popelis [a], Irina Shestakova [a], Mohamed Dammak [c], Viatcheslav Jouikov [d, **]

[a] *Latvian Institute of Organic Synthesis, Aizkraukles 21, Riga, Latvia*
[b] *International College of Cosmetology, Graudu Street 68, Riga, Latvia*
[c] *University of Sfax, Faculty of Sciences, 3000 BP 1171 Sfax, Tunisia*
[d] *UMR 6226 ISCR, University of Rennes-1, 35042 Rennes, France*

ARTICLE INFO

Article history:
Received 30 July 2019
Accepted 4 October 2019
Available online 6 November 2019

Keywords:
Aldimines
Azomethines
Furan
Thiophene
Redox potentials
Cytotoxicity

ABSTRACT

New furan and thiophene derivatives of aldimines *o*-HO-$C_6H_4N{=}CHC_4H_4X(R)$ (X = O, S; R = H, $SiMe_3$, $SiEt_3$, $GeMe_3$, $GeEt_3$) were synthesized by condensation of *o*-aminophenol with the substituted aldehyde precursor. Their structure, electrochemical reduction/oxidation (in CH_3CN/0.1 M Bu_4NPF_6), frontier orbital energies, and cytotoxicity have been studied. Their electrochemical redox potentials E_p show good correlation with the corresponding orbital energies and the difference $E_p^{ox} - E_p^{red}$ corresponds well to their orbital hardness. These new compounds have a pronounced cytotoxicity toward cancer cells of human fibrosarcoma HT-1080 and mouse hepatoma MG-22A ($IC_{50} \cong 1{-}8$ μg ml^{-1}) that can be modulated by introducing a Me_3M substituent into the fifth position of the heterocycle (e.g., $IC_{50}(Me_3Si)/IC_{50}(H) \geq 50$). R_3M-substitution reduces the orbital hardness of the aldimines studied and facilitates oxidation, promoting their oxidative metabolism. The neighboring group effect in the α-Me_3Si-substituted thiophene derivative favors S-oxidation, which supposedly makes its metabolic mechanism different compared to R_3M-substituted furan series (or for M = Ge in the thiophene series). Interestingly, $SiMe_3$ and $GeMe_3$ groups in both heterocyclic series (furan and thiophene) cause opposite trends in cytotoxicity, while the silyl group increases it, the germyl group decreases it.

Motsclés:
Aldimines

RÉSUMÉ

De nouvelles aldimines *o*-HO-$C_6H_4N{=}CHC_4H_4X(R)$ (X = O, S; R = H, $SiMe_3$, $SiEt_3$, $GeMe_3$, $GeEt_3$), dérivées du furanne et du thiophène, ont été synthétisées par la condensation d'*o*-

* Corresponding author.Latvian Institute of Organic Synthesis, Aizkraukles 21, Riga, Latvia.
** Corresponding author.
E-mail addresses: vitalijs@osi.lv (V. Romanovs), vjouikov@univ-rennes1.fr (V. Jouikov).

https://doi.org/10.1016/j.crci.2019.10.002
1631-0748/

Azométhines
Furanne
Thiophène
Potentiels redox
Cytotoxicité

aminophenol avec l'aldéhyde précurseur substitué correspondant. La structure, la réduction et l'oxydation électrochimique (dans CH_3CN/0.1 M Bu_4NPF_6), les énergies des orbitales frontières et la cytotoxicité de ces composés ont été étudiées. Les potentiels redox électrochimiques E_p de ces composés montrent une bonne corrélation avec les énergies orbitalaires correspondantes, et la différence $E_p^{ox} - E_p^{red}$ correspond bien à leur dureté orbitalaire. Ces nouveaux composés ont une cytotoxicité prononcée sur les cellules du fibrosarcome humain HT-1080 et de l'hépatome de souris MG-22A ($IC_{50} \cong 1{-}8$ μg ml^{-1}); elle peut être modulée par l'introduction d'un substituant Me_3M en position 5 de l'hétérocycle (par exemple, $IC_{50}(Me_3Si)/IC_{50}(H) \geq 50$). Cette substitution réduit la dureté orbitalaire des aldimines étudiées et facilite leur oxydation en favorisant le métabolisme oxydatif. L'effet d'un groupe voisin dans le thiophène substitué en position α par Me_3Si favorise son S-oxydation, ce qui vraisemblablement rend son mécanisme métabolique différent par rapport à celui des dérivés R_3M-substitués dans la série du furanne (ou pour M = Ge dans la série du thiophène). Il est intéressant de noter que les groupements $SiMe_3$ et $GeMe_3$ dans les deux séries hétérocycliques (furanne, thiophène) ont des effets opposés sur la cytotoxicité: le groupement silyle l'augmente, tandis que le groupement germyle la réduit.

1. Introduction

Aldimines RCH=NR' are Schiff bases well known in coordination chemistry as mixed-donor ligands [1,2]. However, their chemistry found a much larger use for regioselective and stereoselective reactions, for total synthesis [3], and in preparations of pharmaceutically valuable products [4]. Besides a purely synthetic aspect, redox reactions of aldimines have also been studied, especially during the “golden age” of organic electrochemistry, with polarography being then the main method [5–9].

On the other hand, furan and especially thiophene units are present in many drugs [10]; but—with its evidently important role in their bioactivity—the latter evokes a serious concern about the toxicity of reactive metabolites arising from the oxidation of thiophene-containing biomolecules for humans and animals [11]. Oxidation of thiophenes with CYP isoenzymes family—CYP450 (cytochrome 450), CYP2C9, and others—mainly proceeds via S-oxidation and epoxidation, both processes activating the α-position of the heterocycle and usually leading to an α-hydroxythiophene or a thiolactone. Blocking this site with a neutral, oxidation-stable group might improve the oxidative stability of such compounds and decrease their metabolic toxicity. This idea is supported by the fact that such thiophene-containing drugs as duloxetine, rivaroxaban, and others, in which both α-positions of the thiophene unit are substituted, have no toxicity [12], whereas those with one non-substituted α-position (Methapyrilene, Suprofen, Thienilic acid, OSI-920, and others) are toxic [13–15].

Studying thermochemistry and redox properties using DFT (density functional theory) calculations [16] proved efficient providing meaningful leads to bioactivity of thiophene drugs. Redox properties and biological activity of substrates are often correlated. On the other hand, the introduction of a silyl or a germyl substituent might modulate their redox behavior. Thus, we undertook the present study aiming to prepare several new aldimine derivatives of furan and thiophene (**1a**–**e** and **2a**–**e**) with silyl and germyl substituents. Their bioactivity will then be considered along with their electrochemical properties and supported by DFT modeling.

2. Experimental

Electrochemical measurements were carried out using a PAR 2373 potentiostat operating under PAR PowerSuite software, using a 5-ml glass electrochemical cell in the three-electrode mode. A glassy carbon (GC) disk (2 mm) sealed in a Pyrex tube was used as the working electrode; a 3 × 50 mm GC rod served as the counter electrode. The working electrode was polished consecutively with Struers 2000 and 4000 paper before each run. All potentials, checked using an Fc^+/Fc reversible couple (E^0 = 0.31 V vs

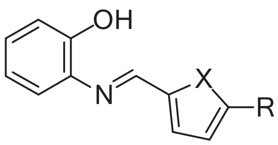

X = O; R = H (**1a**)
$SiMe_3$ (**1b**)
$GeMe_3$ (**1c**)
$SiEt_3$ (**1d**)
$GeEt_3$ (**1e**)

X = S; R = H (**2a**)
$SiMe_3$ (**2b**)
$GeMe_3$ (**2c**)
$SiEt_3$ (**2d**)
$GeEt_3$ (**2e**)

SCE (saturated calomel electrode) [17]), are given against SCE.

DFT calculations (geometry optimization and frequency analysis) were performed using Gaussian 03W (release B.01) program [18] at the B3LYP/Lanl2DZ//HF/6-31G level. Solvation in CH_3CN was accounted for using the Tomasi PCM method [19]. All stationary points were found to be stable global minima as attested by the absence of negative vibration frequencies in harmonic frequency analysis. A scaling factor of 0.98 was applied to B3LYP/Lanl2DZ-calculated IR frequencies [20].

^{1}H and ^{13}C NMR spectra were recorded on a Varian-300 spectrometer (300 and 75 MHz, respectively) in $CDCl_3$, with TMS as the internal standard for ^{1}H and ^{29}Si nuclei and using the residual solvent proton signal (77.05 ppm) for ^{13}C nuclei. Elemental analyses were performed on a CARLO ERBA EA-1108 elemental analyzer. Thin-layer chromatography (TLC) was carried out on Merck silica gel 60 F254 plates. The mass-spectra were recorded under electron impact conditions on a GC-MS Agilent Technologies 7890 GC system with 5975C EI/CI MSD (70 eV) and a capillary column HP-5.

For X-ray analysis, diffraction data were collected at −100 °C on a Bruker-Nonius Kappa CCD diffractometer using graphite monochromatic Mo Kα radiation (λ = 0.71073 Å). The crystal structures of **2b** and **2c** were solved by direct methods and refined by full-matrix least squares. All non-hydrogen atoms were refined in anisotropic approximation. For further details, see crystallographic data for **2b** and **2c** deposited at the Cambridge Crystallographic Data Centre as Supplementary Publication Numbers CCDC 1870490 (for **2b**) and CCDC 1870491 (for **2c**). Copies of the data can be obtained, free of charge, on application to CCDC, 12 Union Road, Cambridge CB2 1EZ, UK.

For the following syntheses, the hetaryl-substituted 2-carbaldehydes have been prepared according to the Dubac procedure [21] treating furan- and thiophenecarbaldehyde with lithium morpholide (aldehyde protection) and *s*-BuLi and then with the corresponding Alk_3MCl (M = Si, Ge).

2-[2-Furylmethyleneamino]-phenol (1a) [22]. A mixture of furan-2-carbaldehyde (0.25 g, 2.3 mmol), 2-aminophenol (0.22 g, 2.3 mmol), and benzene (2 mL) was refluxed for 4 h. The reaction was monitored by TLC using petroleum ether (PE)/Et_2O, 10:0.1. After cooling down, the solvent was evaporated and the residue was dissolved in diethyl ether and dried over $MgSO_4$. The obtained crude product was recrystallized from hexane affording 0.32 g (74%) of pure **1a** as a brown solid. M.p. 62–63 °C (lit. m.p. 68 °C [23]; melting with decomposition at 160–175 °C was reported earlier [24]).

2-[(5-Trimethylsilyl-2-furyl)methyleneamino]-phenol (1b). 5-Trimethylsilyl-furan-2-carbaldehyde (0.39 g, 2.3 mmol) was added to a suspension of 2-aminophenol (0.22 g, 2.3 mmol) in ethanol (10 mL) and the resulting solution was stirred for 14 h at room temperature. The reaction was monitored by TLC (PE/Et_2O, 10:0.1). After evaporation of ethanol, the residue was dissolved in diethyl ether (ca. 10 mL) and dried over $MgSO_4$. After evaporation of ether, the crude product was recrystallized from hexane providing 0.19 g (71%) of pure **1b** as a yellow solid. M.p. 91–92 °C.

^{1}H NMR spectrum (300 MHz, $CDCl_3$), δ, ppm (*J*, Hz): 0.31 (s, 9H, Si–CH_3); 6.78–6.82 (m, 1H); 6.87–6.94 (m, 2H); 7.02–7.13 (m, 2H); 7.16–7.17 (d, 1H); 8.78 (s, 1H); 0.95 (s, 1H, OH). ^{13}C NMR spectrum (75 MHz, $CDCl_3$), δ, ppm: ^{13}C NMR (75 MHz, $CDCl_3$), δ, ppm: −1.77; 115.08; 115.67; 115.73; 119.94; 121.71; 128.67; 135.77; 145.77; 152.34; 156.12; 165.58. ^{29}Si NMR (80 MHz, $CDCl_3$), δ, ppm: −9.55. MS (EI, 70 eV), *m/z* (I_{rel}, %): 259 $[M]^+$ (58); 231 (100); 216 (24); 186 (21); 150 (18); 73 (34); 28 (17). Anal. Calcd ($C_{14}H_{17}NO_2Si$), %: C 64.82; H 6.60; N 5.40. Found, %: C 64.70; H 6.60; N 5.33.

2-[(5-Trimethylgermyl-2-furyl)methyleneamino]-phenol (1c) was prepared similarly to **1b**, reacting 5-trimethylgermyl-furan-2-carbaldehyde (0.49 g, 2.3 mmol) with a suspension of 2-aminophenol (0.22 g, 2.3 mmol) in ethanol (10 mL). After stirring the mixture at room temperature for 4.5 h, the solvent was evaporated and the residue dissolved in diethyl ether to be dried on $MgSO_4$. The crude product obtained after evaporation of ether was recrystallized from hexane affording 0.15 g (66%) of pure **1c** as a light yellow solid. M.p. 94–96 °C.

^{1}H NMR (300 MHz, $CDCl_3$), δ, ppm (*J*, Hz): 0.48 (s, 9H, Ge-CH_3); 6.67–6.68 (d, 1H, *J*=3.3 Hz, H-3); 6.86–6.90 (m, 1H), 6.98–7.02 (m, 2H); 7.14–7.23 (m, 2H); 7.33 (ps, 1H, C–OH); 8.51 (s, 1H). ^{13}C NMR (75 MHz, $CDCl_3$), δ, ppm: −1.88; 114.97; 115.56; 116.09; 119.97; 120.25; 128.59; 135.81; 144.91; 152.34; 155.96; 165.60. MS (EI, 70 eV), *m/z* (I_{rel}, %): 305 $[M]^+$ (23); 277 (31); 186 (100); 158 (22); 119 (14); 28 (55). Anal. Calcd ($C_{14}H_{17}GeNO_2$), %: C 55.32; H 5.64; N 4.61. Found, %: C 55.54; H 5.66; N 4.47.

2-[(5-Triethylsilyl-2-furyl)methyleneamino]-phenol (1d) was prepared similarly to **1b** from 5-triethylsilylfuran-2-carbaldehyde (0.43 g, 2.0 mmol), with stirring for 4.5 h. The recrystallization of the crude product from hexane gave pure **1d** as a brown solid (0.42 g, 69%). M.p. 49–51 °C.

^{1}H NMR (400 MHz, $CDCl_3$, δ, ppm): 0.80–0.89 (m, 6H, Si–CH_2), 1.00–1.01 (m, 9H, Si–CH_2CH_3), 6.86–6.91 (m, 1H), 6.98–7.0 (m, 1H), 7.14–7.18 (m, 2H), 7.65–7.28 (m, 2H), 7.55–7.56 (d, 2H), 8.79 (s, 1H). ^{13}C NMR (75 MHz, $CDCl_3$, δ, ppm): 4.20; 7.26; 114.96; 115.68; 119.99; 128.65; 133.24; 135.21; 135.28; 144.23; 147.29; 149.29; 152.24. ^{29}Si NMR (80 MHz, $CDCl_3$, δ, ppm): 0.98. MS, *m/z* (I, %): 317 (100), 288 (45), 260 (74), 232 (45), 170 (69), 116 (36), 28(87). Anal. Calcd ($C_{17}H_{23}NO_2Si$), %: C 67.73; H 7.69; N 4.64. Found, %: C 67.46; H 7.69; N 4.57.

2-[(5-Triethylgermyl-2-furyl)methyleneamino] phenol (1e) was synthesized similarly to **1b**, using 5-triethylgermylfuran-2-carbaldehyde (0.59 g, 2.3 mmol) and a prolonged (12 h) stirring. Pure **1e** crystallized from hexane as a yellow solid (0.19 g, 66%). M.p. 64–65 °C.

^{1}H NMR (400 MHz, $CDCl_3$, δ, ppm): 1.06–1.16 (m, 15H, Si–CH_2CH_3); 6.83–6.93 (m, 3H); 7.11–7.17 (m, 1H); 7.21–7.23 (m, 1H); 7.38–7.41 (m, 1H); 7.84 (s, 1H); 8.69 (s, 1H). ^{13}C NMR (75 MHz, $CDCl_3$, δ, ppm): 4.44; 8.84; 114.88; 115.45; 115.72; 119.94; 121.41; 128.54; 135.71; 135.73; 144.80; 152.36; 156.16. MS, *m/z* (I, %): 347 (19), 318 (37), 290 (24), 260 (19), 186 (100), 131 (16), 28(89). Anal. Calcd ($C_{17}H_{23}GeNO_2$), %: C 59.01; H 6.70; N 4.04. Found, %: C 59.13; H 6.71; N 3.97.

2-[2-Thienylmethyleneamino]-phenol (2a) was prepared as described for **1a**, using thiophene-2-carbaldehyde (0.26 g, 2.3 mmol). The reaction mixture was refluxed for 4 h. The obtained crude product was recrystallized from hexane affording 0.38 g (55%) of pure **2a** as a brown solid. M.p. 78–79 °C (81 °C [25]).

2-[(5-Trimethylsilyl-2-thienyl)methyleneamino]-phenol (2b) was prepared as described above for **1b**, using 5-trimethylsilyl-thiophene-2-carbaldehyde (0.42 g, 2.3 mmol). The reaction mixture was stirred in ethanol at room temperature for 10 h. Recrystallization from hexane afforded 0.18 g (69%) of pure **2b** as a light yellow solid. M.p. 89–91 °C.

^{1}H NMR spectrum (300 MHz, $CDCl_3$), δ, ppm (J, Hz): 0.37 (s, 9H, Si–CH_3); 6.87–6.91 (m, 1H); 6.99–7.01 (m, 2H); 7.16–7.28 (m, 2H); 7.53–7.54 (d, 1H); 8.78 (s, 1H). ^{13}C NMR (75 MHz, $CDCl_3$), δ, ppm: −0.32; 114.96; 115.64; 119.99; 128.69; 133.26; 134.49; 135.18; 147.26; 147.56; 149.24; 152.24. ^{29}Si NMR (80 MHz, $CDCl_3$), δ, ppm: −5.54. MS (EI, 70 eV), m/z (I_{rel}, %): 275 $[M]^+$ (100); 260 (23); 202 (15); 170 (67); 141 (82); 120 (18); 73 (29); 28(87). Anal. Calcd ($C_{14}H_{17}NOSSi$), %: C 61.14; H 6.23; N 5.09; S 1166. Found, %: C 61.03; H 6.26; N 4.98; S 11.63. Crystal data: monoclinic: a = 6.6387(2), b = 13.4384(5), c = 16.7790(7) Å, β = 91.286(2)°; V = 1496.5(1) Å^3, Z = 4, μ = 0.285 mm^{-1}, D_{calc} = 1.222 g cm^{-3}; and the space group is $P2_1/n$.

2-[(5-Trimethylgermyl-2-thienyl)methyleneamino]-phenol (2c) was prepared as described for **1b**, using 5-trimethylgermyl-thiophene-2-carbaldehyde (0.53 g, 2.3 mmol). The reaction mixture was stirred in ethanol at room temperature for 8 h. Pure **2c** (0.21 g, 63%) was obtained as a light yellow solid with m.p. 88–89 °C.

^{1}H NMR (300 MHz, $CDCl_3$), δ, ppm (J, Hz): 0.51 (s, 9H, Ge-CH_3); 6.86–6.90 (m, 1H); 6.98–7.02 (m, 1H); 7.14–7.28 (m, 3H); 7.53–7.54 (d, 1H); 8.78 (s, 1H). ^{13}C NMR (75 MHz, $CDCl_3$), δ, ppm: −0.59; 114.93; 115.65; 119.99; 128.59; 133.19; 133.39; 135.29; 146.80; 149.18; 149.24; 152.24. MS (EI, 70 eV), m/z (I_{rel}, %): 320 $[M]^+$ (100); 305 (29); 277 (34); 186 (78); 158 (22); 119 (37); 28 (55). Anal. Calcd ($C_{14}H_{17}GeNOS$), %: C 52.54; H 5.36; N 4.38; S 10.02. Found, %: C 52.53; H 5.35; N 4.38; S 10.19. Crystal data: a = 6.6635(2), b = 13.4717(3), c = 16.8383(4) Å, β = 91.045(1)°; V = 1511.30(7) Å^3, Z = 4, μ = 2.153 mm^{-1}, D_{calc} = 1.406 g cm^{-3}; and the space group is $P2_1/n$.

2-[(5-Triethylsilyl-2-thienyl)methyleneamino]-phenol (2d) was prepared similarly to **1d**, using 5-triethylsilylthiophene-2-carbaldehyde (0.52 g, 2.3 mmol) and stirring the mixture for 9 h. After recrystallization from hexane, pure **2d** was obtained as a light yellow solid (0.26 g, 71%). M.p. 67–69 °C.

^{1}H NMR (400 MHz, $CDCl_3$, δ, ppm): 0.79–0.87 (m, 6H, Si–CH_2), 1.00–1.01 (m, 9H, Si–CH_2CH_3), 6.76–6.77 (m, 1H), 6.85–6.90 (m, 1H), 6.98–7.02 (m, 2H), 7.14–7.27 (m, 2H), 7.38 (s, 1H), 8.53 (s, 1H). ^{13}C NMR (75 MHz, $CDCl_3$, δ, ppm): 3.05; 7.23; 115.03; 115.36; 115.58; 119.94; 122.79; 128.67; 135.69; 144.99; 152.37; 156.28; 163.78. ^{29}Si NMR (80 MHz, $CDCl_3$, δ, ppm): −2.36. MS, m/z (I, %): 301 (88), 273 (90), 242 (100), 214 (69), 186 (45), 164 (36), 107(61), 59 (42). Anal. Calcd ($C_{17}H_{23}NOSSi$), %: C 64.30; H 7.30; N 4.41; S 10.10. Found, %: C 64.42; H 7.36; N 4.28; S 10.29.

2-[(5-Triethylgermyl-2-thienyl)methyleneamino] phenol (2e). Using 5-triethylgermylthiophene-2-carbaldehyde (0.62 g, 2.3 mmol) as a starting compound and the same protocol as for **2c** and stirring the solution for 14 h, pure **2e** was obtained after the recrystallization form hexane as a yellow solid with 69% yield (0.21 g). M.p. 68–69 °C.

^{1}H NMR (400 MHz, $CDCl_3$, δ, ppm): 1.05–1.15 (m, 15H, Si–CH_2CH_3), 6.85–6.90 (m, 1H), 6.98–7.01 (m, 1H), 7.13–7.19 (m, 3H), 7.24–7.27 (m, 1H), 7.54–7.56 (d, 1H), 8.78 (s, 1H). ^{13}C NMR (75 MHz, $CDCl_3$, δ, ppm): 5.43; 8.82; 114.91; 115.66, 119.99, 128.53; 133.22; 134.15; 135.38; 146.06; 146.85; 149.31; 152.20. MS, m/z (I, %): 363 (59), 334 (97), 306 (21), 276 (17), 202 (18), 170 (100), 139(49), 97 (43), 28 (91). Anal. Calcd ($C_{17}H_{23}GeNOS$), %: C 56.39; H 6.40; N 3.87; S 8.86. Found, %: C 56.48; H 6.36; N 3.78; S 8.97.

3. Results and discussion

3.1. Synthetic approach

Aldimines **1a–e** and **2a–e** were prepared by condensation of 2-aminophenol with the corresponding aldehyde in refluxing benzene (Scheme 1). However, refluxing in this solvent (even for 40 h) turned out to be poorly suitable for preparing trimethylsilyl(germyl)-substituted furan and thiophene aldimines: the aldehyde did not react completely and the attempts to recrystallize the product from the reaction mixture led to its decomposition. Changing the reaction conditions (stirring in ethanol at room temperature for 4.5–14 h) allowed us to obtain trimethylsilyl(germyl)-substituted aldimines with 63–71% yields.

3.2. Structural features

The structure of the compounds **2b** and **2c** was confirmed by X-ray diffraction analysis (Figs. 1 and 2). The crystal structures of **2b** and **2c** are isomorphous. Their molecular structures are characterized by strong intramolecular hydrogen bonds of the OH···N type pointing the OH group toward the azomethine bridge. The corresponding lengths of this contact are 2.617(2) Å (H···N = 2.05(2) Å and ∠O–H···N = 124(2)°) for **2b** and 2.621(2) Å (H···N = 2.06(3) Å and ∠O–H···N = 128(2)°) for **2c**. In the crystal state, these hydrogen bonds are bifurcated forming additional OH···O type intermolecular bonds between the neighboring molecules. The lengths of these intermolecular bonds are 2.938(2) Å (H···O = 2.48(2) Å and ∠O–H···O =

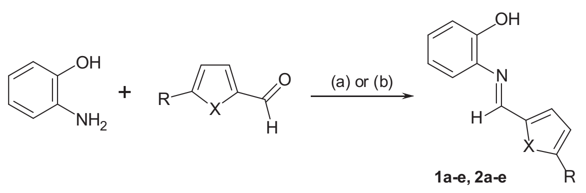

Scheme 1. Synthesis of aldimines **1a–e** and **2a–e.** (a) For **1a**, **2a**: benzene, 80 °C, (b) for **1b–e** and **2b–e**: EtOH, rt.

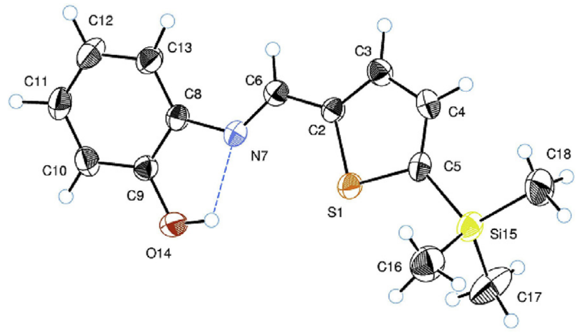

Fig. 1. ORTEP structure of 2-[(5-trimethylsilyl-2-thienyl)methyleneamino]phenol (**2b**). Thermal ellipsoids are shown with 50% probability. The intramolecular OH···N hydrogen bond is shown with a dotted line. Selected geometrical parameters: N–C(6) = 1.279(4) Å, N–C(8) = 1.412(6) Å, C(6)–C(2) = 1.442(9) Å, Si–C(18) = 1.851(6) Å, Si–C(16) = 1.858(4)Å, ∠C(8)–N–C(6)–C(2) = 175.61°, ∠N–C(6)–C(2)–S = 1.07°, ∠S–C(5)–Si–C(18) = 179.76°.

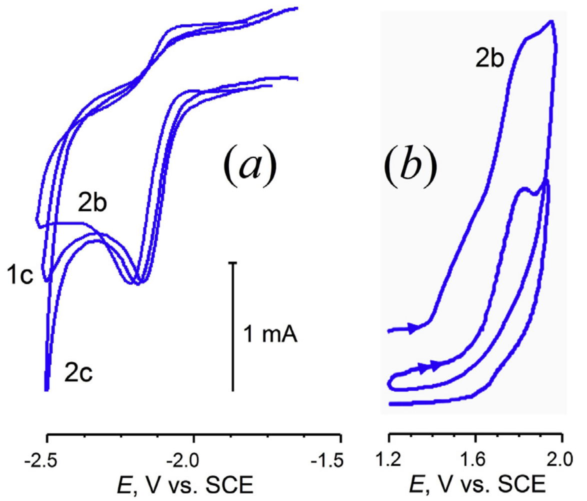

Fig. 3. Voltammograms of (a) reduction of **1c**, **2b**, and **2c**, and (b) oxidation of **2b** (first and second cycles) in CH_3CN/0.1 M Bu_4NPF_6 at a GC disk electrode. Scan rate $v = 0.2$ V s^{-1}. $T = 20$ °C.

115(2)°) for **2b** and 2.934(2) Å (H···O = 2.52(2) Å and ∠O–H···O = 114(2)°) for **2c**.

In both structures, the N=C azomethine fragment is not distorted (∠NC_6C_2 = 121.08° and ∠C_8NC_6 = 122.25° in **2b**, whereas in **2c**, these angles are 120.85° and 122.28°, correspondingly) and is coplanar to the thiophene unit (dihedral angles ∠N–C–C–S are 1.07° and 1.89° for **2b** and **2c**, respectively). However, phenyl and thiophene rings are twisted with respect to each other by ca. 18° (the dihedral ∠$C_{13}C_8NC_6$ in **2b** and its equivalent in **2c** are 18.18° and 17.79°, respectively) which somewhat disturbs their ring-to-ring π-conjugation. In the absence of obvious electronic reasons for this, the energy causing this twist visibly arises from *ortho*-repulsion between the C–H protons of phenyl and azomethine units. In fact, though σ(C_3–H) and σ(C_6–H) bonds in **2b** are eclipsed and practically parallel (same for σ(C_{10}–H) and σ(C_4–H) in **2c**), they are quite distant (H···H = 2.715(2) Å (**2b**) and 2.681(7) Å (**2c**)), whereas the phenyl C_{13}–H and methine C_6–H protons are closer (H···H = 2.379(2) Å and 2.100(8) Å for **2b** and **2c**, respectively) forming an open six-membered structure (Figs. 1 and 2).

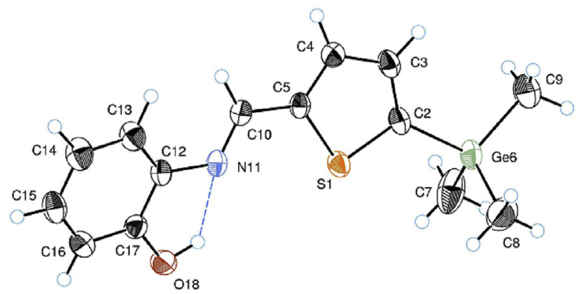

Fig. 2. ORTEP drawing of 2-[(5-trimethylgermyl-2-thienyl)methyleneamino]phenol (**2c**). Thermal ellipsoids are shown with 50% probability. The intramolecular OH···N hydrogen bond is shown with a dotted line. Selected geometrical parameters: N–C(12) = 1.415(1) Å, N–C(10) = 1.272(8) Å, C(6)–C(2) = 1.443(6) Å, Ge–C(9) = 1.933(3) Å, Ge–C(7) = 1.937(3)Å, ∠C(12)–N(11)–C(10)–C(5) = 174.93°, ∠N–C(10)–C(5)–S = 1.89°, ∠S–C(2)–Ge–C(9) = 179.98°.

Remarkably, the M–$C_{thienyl}$ bond in both **2b** (M = Si, Si–C_5 = 1.874(2) Å) and **2c** (M = Ge, Ge–C_2 = 1.946(9) Å) is longer than the three other M-C bonds, and one of these three M-C bonds (eclipsed M-Me) is ca. 0.003–0.004 Å shorter than the other two (e.g., Ge–C_9 = 1.933(3) Å and Ge–C_7 = 1.937(3) Å, Fig. 2). This feature attests to an additional π–$σ_{(C\text{-}M)}$-type hyperconjugation of the Me_3M groups with the heterocycle in both **2b** and **2c** which overcomes the repulsion energy of the eclipsed σ-bonds in the practically planar H–C(3)–C(2)–Ge–C(9) fragment (∠SC_2GeC_9 = 179.98°).

The structure of the synthesized aldimines was also confirmed by the ^{1}H NMR, ^{13}C NMR, and ^{29}Si NMR (for **1b** and **2b**) spectroscopy.

3.3. Electrochemical study

The known electrochemical data on aldimines were obtained mostly in acidic or basic media, at pH rarely met in biological systems [7,9,26]. In addition, these compounds are not stable under such conditions. In aqueous media with pH even moderately different form neutral, their redox processes are complicated by acid–base interactions depending, besides their chemical structures, on different factors (concentration, proton activity, supporting electrolyte, etc. [8]). The redox reactions following first electron transfer (ET) usually produce highly reactive intermediates (ions or radical ions very improbably to be formed in biological processes [26]); otherwise they concern secondary stable products resulting from the initial electron release/uptake. When R is a good leaving group, the reduction of the >C=N–R unit might result in the N–R bond scission leading to a corresponding nitrile [27,28] and an RH compound so that the immediate biological effect might be anticipated knowing the nature of these products. The oxidation of aldimines in aqueous solutions or in wet organic media involves the N=C bond cleavage as well, leading through the formation of a protonated anisidine to

Table 1
Reduction and oxidation potentials E_p (V vs SCE), peak half-widths ($\Delta E_{p\text{-}p/2}$, mV),[a] frontier orbital energies (ε, $\Delta\varepsilon$, eV),[b] and dipole moments (μ, D)[b] of **1a**–**e** and **2a**–**e**.

Cpd	Reduction			Oxidation			μ	ΔE_p [c]	$\Delta\varepsilon$ [d]
	E_p^{red}	$\Delta E_{p\text{-}p/2}$	$-\varepsilon_{LUMO}$	E_p^{ox}	$\Delta E_{p-p/2}$	$-\varepsilon_{HOMO}$			
1a	−2.169	75	2.327	1.879	95	6.019	6.22	4.048	3.693
1b	−2.149	76	2.160	1.756	88	5.722	4.06	3.905	3.562
1c	−2.140	84	2.136	1.761	90	5.702	4.07	3.901	3.566
1d	−2.142	80	2.128	1.753	85	5.689	4.01	3.895	3.561
1e	−2.138	76	2.100	1.752	80	5.664	4.02	2.890	3.563
2a	−2.185	89	2.371	1.834	>110	5.870	4.07	4.019	3.500
2b	−2.180	80	2.309	1.782	>130	5.778	4.22	3.962	3.468
2c	−2.168	75	2.285	1.803	90	5.759	4.29	3.971	3.474
2d	−2.168	72	2.274	1.783	80	5.744	4.28	3.469	3.469
2e	−2.166	78	2.248	1.767	82	5.722	4.38	3.933	3.474

[a] At GC electrode in CH_3CN/0.1 M Bu_4NPF_6.
[b] From DFT B3LYP/Lanl2DZ//HF/6-31G calculations.
[c] $\Delta E_p = E_p^{ox} - E_p^{red}$.
[d] $\Delta\varepsilon = \varepsilon_{HOMO} - \varepsilon_{LUMO}$.

the corresponding aldehyde and the quinone imine [29]. Therefore, only first redox steps might be considered as characteristic of biological relevance of aldimines as such.

At a fixed R (o-C_6H_4OH), electron affinity and ionization of the π-system of aldimines are the prime factors in their redox activity [9], so we considered first redox potentials of the reaction series **1a**–**e** and **2a**–**e** and the energies of the frontier orbitals (FO) corresponding to these processes.

At a Pt electrode in CH_3CN/0.1 M Bu_4NPF_6, the voltammograms of **1a**–**e** and **2a**–**e** are irreversible and poorly reproducible because of electrode passivation. At a glassy carbon (GC) electrode, the curves were better shaped (Fig. 3) albeit some accompanying peaks appeared upon scanning because of the propensity of these compounds to adsorption and electropolymerization [30]. The oxidation potentials are close to those reported (in CH_2Cl_2/0.1 M Bu_4NClO_4) for structurally related thiophene(furan) bis-substituted phenyl aldimines [31]. The i_p peak currents of both oxidation and reduction steps are diffusion-controlled as follows from their linear dependence on the concentration and scan rate ($i_p/Cv^{1/2}$ = const). The reduction peak half-widths ($\Delta E_{p-p/2} = E_p - E_{p/2}$, Table 1) are broadened in both series over 58 mV typical for electrochemically reversible processes [32]. Supposedly, this is not due to a slow ET because the kinetic shift of the E_ps of **1a**–**e** and **2a**–**e** with the scan rate ($\Delta E_p/\Delta\ln(v) \cong$ 35–40 mV) remains close to 30 mV per decade of v, corresponding to a EC mechanism with a fast first-order reaction following ET [32]. This trend is also supported by somewhat larger oxidation peaks (higher $\Delta E_{p\text{-}p/2}$, Table 1) because of preferential adsorption of thiophene at anodic potentials [33]. The redox characteristics of **1a**–**e** and **2a**–**e** in reduction and oxidation processes are collected in Table 1.

The E_ps of both processes are clearly affected by the nature of the heteroaromatic unit at the methine carbon and by the substituent at its α-position, though the last effect is modest. Indeed, the $GeMe_3$ group in aromatic systems exerts the same polar substituent effect as H (i.e. σ_p = 0 [34]), while $SiMe_3$ acts as a weak donor ($\sigma_p = -0.07$) [34]. Of 2-furyl and 2-thienyl substituents, the former is slightly less acceptor (σ_p = 0.02 and 0.05, respectively [34])

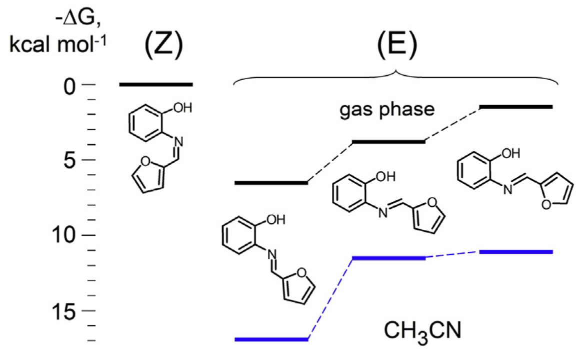

Fig. 4. Relative free energies of formation of the different forms of 2-(furan-2-ylmethyleneamino)-phenol **2a**. In blue: values in CH_3CN. From DFT B3LYP/Lanl2DZ (CPM) calculations.

though the whole effect is rather small. A similar trend is true for the additive inductive constants of these groups (σ^* = 1.11 and 1.28) [35]. Thus, the resulting influence of R in **1a**–**c** and **2a**–**c** is distinct but rather small to cause a dramatic differentiation in their redox properties.

These molecules are quite polar (dipole moment μ = 4.06…6.22 D), yet this parameter follows different trends in series **1a**–**c** and **2a**–**c**. Interestingly, most polar derivatives **1a** and **2c** seem to have more pronounced biological activity (see Section 3.5).

3.4. DFT modeling

Experimental electrochemical quantity $E_p^{ox} - E_p^{red}$ ($E_0^{ox} - E_0^{red}$ in the case of purely reversible processes) reflects the fundamental orbital quantity, the HOMO–LUMO energy difference,* which characterizes chemical "hardness" of a molecule [39]. Both quantities are directly linked

* Strictly speaking, E_p is not an equivalent of E_0, because it is shifted with respect to E_0 by the ensuing chemical reaction ("kinetic shift") [32]. However, this shift is often constant or linear with E_0, so that using E_p instead of E_0 might often be a good approach; see Refs. [36–38].

to its donor–acceptor ability that can be considered in terms of nucleo/electrophilicity or acido-basicity [40,41], the parameters closely related to biological activity [42,43]. However, the comparison of the experimental redox data with orbital energies is only possible using right geometry for the FO energy calculations because the conjugation in planar systems **1a**–**e** and **2a**–**e** is very sensitive to structural factors. The (*E*)-form of **1a** is more favorable over its (*Z*)-form with the planes of C_6H_4OH and furan units helix-wise twisted out of the common plane by strong *ortho*-repulsion, $\Delta G[\mathbf{1a}(E) - \mathbf{1a}(Z)] = -6.44$ kcal mol^{-1} (DFT B3LYP/Lanl2DZ), and this is the form that was actually formed, in agreement with X-ray data. Important intramolecular N•••H interaction in **1a** stabilizes this system by 20.4 kcal mol^{-1} compared to a non-coordinated structure. On the potential energy curve of (*E*)-2-(furan-2-ylmethyleneamino)phenol, three minima are marked. The form with σ-trans position of N and O(furan) atoms, where all three chelating centers (O, N, O) are pointed to the same direction, while the azomethine C–H bond is turned to the opposite side, corresponds to the global minimum in the gas phase and in CH_3CN solution; two other (E)-forms are local minima with higher energy (Fig. 4). A similar configuration is found to be the global minimum for **2a** as well.

This configuration is in agreement with the experimental IR spectra of **1a** and **2a**. A broad band at $\nu_{O-H} = 3000$ cm^{-1} is due to the vibration of the OH hydrogen involved in the intramolecular coordination with N atom [44]. Respectively, the ν_{C-O} band now appears at 1472 cm^{-1}, and a characteristic Schiff base $\nu_{C=N}$ band [45] is shifted to lower frequencies ($\nu = 1634$ cm^{-1}) because of N•••H coordination (cf. X-ray structures of **2b** and **2c**, Figs. 1 and 2). The methine C–H bond in **1a** and **2a** vibrates with a practically similar frequency typical for this conformation ($\delta_{C-H} = 3035$ cm^{-1}), which is well reproduced by DFT calculations (Fig. 5).

The frontier orbitals (FOs) (Fig. 6) are quite similar in the reaction series **1** and **2**, with the main difference arising from the orbital coefficients of O and S in the heteroaromatic rings. Remarkably, Me_3Si and Me_3Ge substituents

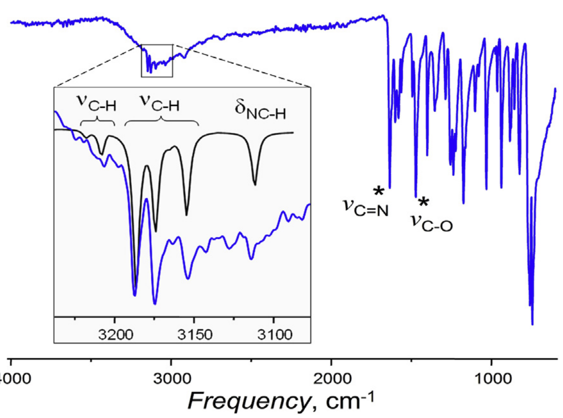

Fig. 5. IR spectrum of **1a**. In the inset, appearing on the large ν_{O-H} band, are DFT-calculated (black) IR frequencies of aromatic C–H bonds in furan (left group) and phenol (right group), and of the methine (N=)C–H carbon–proton bond.

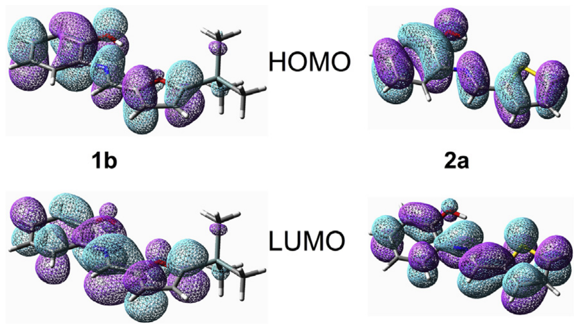

Fig. 6. Redox-related frontier orbitals (HOMO and LUMO) of **1b** and **2a** (from DFT B3LYP/Lanl2DZ calculations).

do not strongly perturb these orbital features: neither Si nor Ge are directly involved in these FO, the substituents are mostly contributing through hyperconjugation of their $M-C_{sp3}$ (M = Si, Ge) bonds with the π-electron system (Fig. 6) in agreement with what was observed by X-ray diffractometry (Figs. 1 and 2).

Fig. 7 thus shows the E_p^{ox} and E_p^{red} plotted against the corresponding FO energies and the correlation of ($E_p^{ox} - E_p^{red}$) with the $\varepsilon_{HOMO} - \varepsilon_{LUMO}$ difference. In both families, **1a**–**e** and **2a**–**e**, E_p^{ox} – IP and $E_p^{red} - \varepsilon_{LUMO}$ are well correlated, forming common plots, though their less than unity slopes ($\Delta E_p^{ox}/\Delta IP = 0.38$ and $\Delta E_p^{red}/\Delta\varepsilon_{LUMO} = 0.18$) indicate a strong influence of the chemical reaction following the first ET on the experimental E_ps (large kinetic shift). Quite similar trends were previously found for furyl and thienyl nitrones and nitroethenes [36]. When considered in terms of orbital hardness, furyl- and thienyl-substituted aldimines form two different groups (Fig. 7, c). Interestingly, charge-based isotropic dipole moments μ of **1a**–**e** and **2a**–**e**, reflecting their polarity, are distinctly in line with each of the orbital energies, ε_{HOMO} and ε_{LUMO} (Table 1), but they loose the selectivity for their difference and are no more specific for properties correlations.

3.5. *Cytotoxicity and toxicity*

Aldimines and their derivatives possess a broad spectrum of biological activity, such as anti-bacterial, anti-cancer [46], anti-fungal (*Candida albicans* and *Aspergillus niger*) [4], anti-inflammatory, anti-virus, anti-pyretic [47], and a significant activity against *Staphylococcus aureus* and epidermidis, *Bacillus subtilis* and cereus, *Micrococcus luteus*, and *Escherichia coli*. Their complexes with metals (e.g., Cu, Ni, Zn) showed very good activity against leukemia cells (CEM-SS) [4].

The in vitro cytotoxicity of heteroaryl-substituted aldimines **1a**–**e** and **2a**–**e** was investigated for two tumor lines, HT-1080 (human fibrosarcoma) and MG-22A (mouse hepatoma), and on normal mouse fibroblasts NIH 3T3 to determine the effect of the substituent at the fifth position and of the type of heterocycle on antitumor activity. The results of experimental evaluation of the cytotoxic properties are presented in Table 2.

The aldimines **1a** and **1c** have high cytotoxic activity (IC_{50} 1–8 μg ml^{-1}) on both cancer cell lines and also have

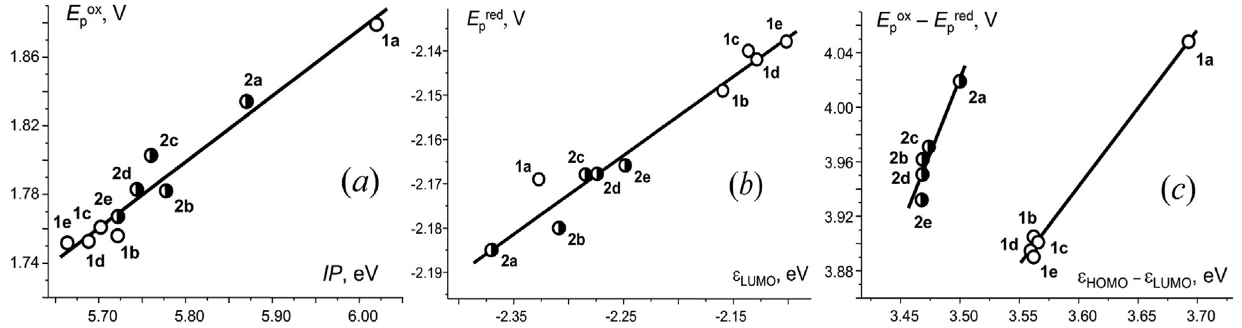

Fig. 7. Correlations of (a) E_p^{ox} with the first ionization potential (IP = -ε_{HOMO}); (c) E_p^{red} with LUMO energy; (c) the difference in first redox potentials ($E_p^{ox} - E_p^{red}$) with the $\varepsilon_{HOMO} - \varepsilon_{LUMO}$ difference.

high cytotoxic effect on NIH 3T3 cells (IC_{50} 1–9 μg ml^{-1}). The introduction of the Me_3M substituent to the heterocycle has a special effect in both O and S series. In the furan series, the silylated aldimine **1b** generally shows a decrease in both cytotoxicity and toxicity. Its thiophene analogue **2b** shows better cytoselectivity: it has higher cytotoxicity on cancer cell line MG-22A (IC_{50} 6 μg ml^{-1}) than on HT-1080 (IC_{50} 26 μg ml^{-1}) but unlike other aldimines of this family, this compound is very toxic (LD_{50} 4 mg kg^{-1}). Me_3Ge-substituted **2c** is more promising here as it has practically similar cytotoxicity as non-substituted **2a** but with reduced toxicity. Aldimine **1d** has most pronounced cytotoxicity in these series for both HT-1080 and NIH 3T3 cells but at the same time, it is quite toxic, LD_{50} < 60 mg kg^{-1}. In contrast, its thiophene analogue **2d** is the less toxic (Table 1), although also less efficient against the two tumor lines and NIH 3T3. Et_3Ge-substituted furan derivative **1e** has a good cytotoxicity toward NIH 3T3 at rather high LD_{50}, but it is less selective for HT-1080 and MG-22A tumor cells.

Remarkably, in the corresponding series, the oxidation E_ps of both Me_3Si derivatives, **1b** and **2b**, are lower than those of non-substituted **1a** and **2a** (Table 1). However, while the α-Me_3Si group promotes (for the Me_3Si neighboring group effect, see, e.g., Ref. [48]) the S-oxidation, similar to the oxidation by cytochrome CYP450 [16], the oxidation of the furan derivative is not O-centered and follows a different way. We venture to suppose that the acute toxicity of **2b** might be related to its easier metabolic S-oxidation leading to toxic products [11,16]. The parent α-Me_3Ge group in **2c** is less conjugated with the π-system of the heterocycle because of the size mismatch of its more diffuse $\sigma_{(C-Ge)}$ orbitals responsible for the electronic effects, so probably its overall action results from different factors (solubility, coordination of Ge with biological phosphates, etc.). Interestingly, when the Me_3Si group increases the toxicity, the Me_3Ge group induces the opposite trend.

Overall, aldimines **1a**, **2a**, and **2c** seem to have the most advantageous combination of biological properties, thus providing good leads for the further development in these reaction series.

Table 2
In vitro cytotoxicity (IC_{50}) and toxicity (LD_{50}) of aldimines **1a**–**e** and **2a**–**e**.

Compound	IC_{50}, μg ml^{-1}			LD_{50}, mg·kg^{-1}
	HT-1080	MG-22A	NIH 3T3	
	MTT[a]	MTT	NR	
1a	2	1	9	187
1b	>100	30	11	259
1c	3	8	1	91
1d	0.2	2	<0.3	<60
1e	24	21	5	232
2a	10	8	12	144
2b	26	6	193	4
2c	18	12	15	192
2d	56	12	43	483
2e	21	25	17	398

[a] Coloration indicators: MTT = 3-(4,5-dimethylthiazol-2-yl)-2,5-diphenyl-2H-tetrazolium bromide, NR = neutral red.

4. Conclusion

To conclude, new aldimine derivatives of *o*-aminophenol, with furanyl and thiophenyl substituents (C_4H_4X, X = H, $SiAlk_3$, $GeAlk_3$, with Alk = Me, Et) were synthesized through a simple procedure condensing the aniline with the corresponding precursor aldehyde. The structure of these new products as well as redox properties in CH_3CN/0.1 M Bu_4NPF_6, their frontier orbital energies, cytotoxicity, and toxicity have been considered. Their electrochemical redox potentials E_p show good correlation with the related orbital energies and the difference $E_p^{ox} - E_p^{red}$ corresponds well to the orbital hardness of these compounds. Me_3Si and Me_3Ge substitution of the heterocycle facilitates the oxidation of the corresponding molecules (promoting their oxidative metabolism), and—though not being dramatical—alters their redox properties. However, remarkably reducing their orbital hardness, Me_3M substitution can also substantially affect solubility and hydro(phobicity/philicity) and hydrogen-bonding ability of these molecules. The steric hindrance of both Me_3M groups is relatively small because of longer C–Si and C–Ge bonds compared to C–C; this same feature accounts for attenuating their electronic interaction (hyperconjugation) with the aldimine π-system, especially for the Me_3Ge group. To the overall effect of this latter, additional factors add such as more diffuse conjugating $\sigma_{(C-Ge)}$ orbital and longer Ge–C(H_3) bonds, making Ge more available for external coordination and nucleophilic interactions.

The new aldimines have shown a pronounced cytotoxicity toward cancer cells of human fibrosarcoma HT-1080 (with IC_{50} as low as 0.2–3 μg ml^{-1}) and of mouse hepatoma MG-22A (IC_{50} ≅ 1–8 μg ml^{-1}). Their cytotoxicity can be largely modulated by the Me_3M substituent to the fifth position of the heterocycle, up to 50 times in furan series and to 3–5 times for thiophene derivatives. For electronic reasons, the α-Me_3Si substituent exerts a strongest neighboring group effect when attached to the thiophene unit. As a consequence, it enhances the oxidation on the S atom thus altering the oxidative metabolism of this compound, which is translated by its acute toxicity. In other cases, toxicity generally decreases upon R_3M substitution, though Et_3Si and Me_3Ge derivatives in the furan series fall out of this trend. Further works in this field are in progress.

Acknowledgments

The authors gratefully acknowledge the support of this research by the Latvian Council for Science (Project 225/2012) and from PHC OSMOSE #39669QC.

References

[1] B.O. West, in: E.A.V. Ebsworth, A.G. Madock, A.G. Shappe (Eds.), New Pathways in Inorganic Chemistry, Cambridge University Press, London, 1968, p. 303.
[2] R.K. Pardeshi, Coordination Chemistry of Schiff Bases: Metal–Ligand Complexes, Lambert Academic Publishing, 2016.
[3] S. Patai (Ed.), Carbon-Nitrogen Double Bonds, Patai's Chemistry of Functional Groups, John Wiley & Sons, Inc., NY, 1970.
[4] R. Sahu, D.S. Thakur, P. Kashyap, Int. J. Pharm. Sci. Nanotechnol. 5/3 (2012) 1757–1764.
[5] L. Eberson, K. Nyberg, in: A.J. Bard, H. Lund (Eds.), Enyclopedia of Electrochemistry of the Elements, vol. 12, Marcel Dekker, NY, 1978, 261-238.
[6] Y.P. Kitaev, T.V. Troepolskaya, in: A.N. Frumkin, A.B. Ershler (Eds.), Progress in Electrochemistry of Organic Compounds 1, Plenum Publishing Co., Ltd, NY, 1971, pp. 43–83.
[7] T.V. Troepolskaya, G.K. Budnikov, Electrochemistry of Azomethines, Nauka, Moscow, 1989, p. 216.
[8] H. Lund, in: S. Patai (Ed.), Carbon-Nitrogen Double Bonds, Patai's Chemistry of Functional Groups, John Wiley & Sons, Inc., NY, 1970, p. 505.
[9] H. Lund, in: H. Lund, O. Hammerich (Eds.), Organic Electrochemistry, 4th ed., Marcel Dekker, New York, 2001, p. 435.
[10] M. Krátký, J. Vinsova, Curr. Top. Med. Chem. 26 (2016) 2921–2952.
[11] D. Gramec, L.P. Masic, M.S. Dolenc, Chem. Res. Toxicol. 27 (2014) 1344–1358.
[12] C. Weinz, T. Schwarz, D. Kubitza, W. Mueck, D. Lang, Drug Metab. Dispos. 37 (2009) 1056–1064.
[13] E.E. Graham, R.J. Walsh, C.M. Hirst, J.L. Maggs, S. Martin, M.J. Wild, I.D. Wilson, J.R. Harding, J.G. Kenna, R.M. Peter, D.P. Williams, B.K. Park, J. Pharmacol. Exp. Ther. 326 (2008) 657–671.
[14] J.P. O'Donnell, D.K. Dalvie, A.S. Kalgutkar, R.S. Obach, Drug Metab. Dispos. 31 (2003) 1369–1377.
[15] C. Medower, L. Wen, W.W. Johnson, Chem. Res. Toxicol. 21 (2008) 1570–1577.
[16] C.K. Jaladanki, N. Taxak, R.A. Varikoti, P.V. Bharatam, Chem. Res. Toxicol. 28/12 (2015) 2364–2376.
[17] C.K. Mann, K.K. Barnes, Electrochemical Reactions in Nonaqueous Systems, Marcel Dekker, NY, 1970, p. 403.
[18] M.J. Frisch, G.W. Trucks, H.B. Schlegel, G.E. Scuseria, M.A. Robb, J.R. Cheeseman, J.A. Montgomery Jr., T. Vreven, K.N. Kudin, J.C. Burant, J.M. Millam, S.S. Iyengar, J. Tomasi, V. Barone, B. Mennucci, M. Cossi, G. Scalmani, N. Rega, G.A. Petersson, H. Nakatsuji, M. Hada, M. Ehara, K. Toyota, R. Fukuda, J. Hasegawa, M. Ishida, T. Nakajima, Y. Honda, O. Kitao, H. Nakai, M. Klene, X. Li, J.E. Knox, H.P. Hratchian, J.B. Cross, C. Adamo, J. Jaramillo, R. Gomperts, R.E. Stratmann, O. Yazyev, A.J. Austin, R. Cammi, C. Pomelli, J.W. Ochterski, P.Y. Ayala, K. Morokuma, G.A. Voth, P. Salvador, J.J. Dannenberg, V.G. Zakrzewski, S. Dapprich, A.D. Daniels, M.C. Strain, O. Farkas, D.K. Malick, A.D. Rabuck, K. Raghavachari, J.B. Foresman, J.V. Ortiz, Q. Cui, A.G. Baboul, S. Clifford, J. Cioslowski, B.B. Stefanov, G.L.A. Liashenko, P. Piskorz, I. Komaromi, R.L. Martin, D.J. Fox, T. Keith, M.A. Al-Laham, C.Y. Peng, A. Nanayakkara, M. Challacombe, P.M.W. Gill, B. Johnson, W. Chen, M.W. Wong, C. Gonzalez, J.A. Pople, Gaussian 03, Revision B.01, Gaussian, Inc., Pittsburgh PA, 2003.
[19] J. Tomasi, B. Mennucci, R. Cammi, Chem. Rev. 105 (2005) 2999.
[20] D.C. Young, Computational Chemistry: a Practical Guide for Applying Techniques to Real-World Problems, John Wiley & Sons, Inc., NY, 2001.
[21] F. Denat, H. Gaspard-Iloughmane, J. Dubac, Synthesis 10 (1992) 954–956.
[22] N.K. Chaudhary, Arch. Appl. Sci. Res. 5/6 (2013) 227–231.
[23] E. Tauer, J. Org. Chem. 46/21 (1981) 4252–4258.
[24] G. Fenech, Ann. Chim. 44 (1954) 324–329.
[25] G.L. Eichhorn, J.C. Bailar Jr., J. Am. Chem. Soc. 75 (1953) 2905–2907.
[26] J.M.W. Scott, W.H. Jura, Can. J. Chem. 45 (1967) 2375.
[27] F.D. Popp, H.P. Schultz, Chem. Rev. 62 (1962) 19.
[28] J.P. Coleman, in: S. Patai (Ed.), The Chemistry of Acid Derivatives, Suppl B, Wiley-Interscience, NY, 1979, pp. 782–824.
[29] J.K. Leland, M.J. Powell, J. Electrochem. Soc. 137 (1990) 3127.
[30] F. Brovelli, B.L. Rivas, J.C. Bernède, J. Chil. Chem. Soc. 50 (2005) 597–602.
[31] C.I. Simionescu, I. Cianga, M. Ivanoiu, Al Duca, I. Cocarla, M. Grigoras, Eur. Polym. J. 35 (1999) 587–599.
[32] O. Hammerich, in: H. Lund, O. Hammerich (Eds.), Organic Electrochemistry, 4th ed., Marcel Dekker, NY, 2001, p. 109.
[33] V. Jouikov, J. Simonet, in: A. Bard, M. Stratman, H. Shaefer (Eds.), Encyclopedia of Electrochemistry, vol. 8, Wiley-VCH, New York, 2004, p. 235.
[34] C. Hansch, A. Leo, R.W. Taft, Chem. Rev. 97 (1991) 165–195.
[35] A.R. Cherkasov, V.I. Galkin, R.A. Cherkasov, Russ. Chem. Rev. 65 (1996) 695–711.
[36] M. Boulkroune, L. Ignatovich, V. Muravenko, J. Spura, A. Chibani, V. Jouikov, Chem. Heterocycl. Comp. 11 (2013) 1706–1715.
[37] S. Soualmi, L. Ignatovich, E. Lukevics, A. Ourari, V. Jouikov, J. Organomet. Chem. 693 (2008) 1346–1352.
[38] V.F. Sidorkin, E.F. Belogolova, Y. Wang, V. Jouikov, E.P. Doronina, Chem. Eur J. 8 (2017) 1910–1919.
[39] R.G. Pearson, Chemical Hardness, Wiley-VCH, Weinheim, 1997, p. 27.
[40] G. Klopman, J. Am. Chem. Soc. 90 (1968) 223.
[41] G. Klopman (Ed.), The Reactivity and Reaction Pathways [Russ. Transl, Mir, Moscow, 1977, p. 383.
[42] D.L. Nelson, M.M. Cox, Lehninger Principles of Biochemistry, W.H. Freeman and Co., New York, 2005, p. 157.
[43] H.F. Gilbert, Basic Concepts in Biochemistry, 2nd ed., McGraw-Hill Co., Inc., 2000, p. 304.
[44] M. Nath, N. Chaudhary, Synth. React. Inorg. Met. Org. Chem. 28 (1998) 121–133.
[45] H.H. Freedman, J. Am. Chem. Soc. 83 (1961) 2900.
[46] A. Rani, M. Kumar, R. Khare, H.S. Tuli, J. Biol. Chem. Sci. 2/1 (2015) 62–91.
[47] A.M. Abu-Dief, I.M.A. Mohamed, J. Basic Appl. Sci. 4 (2015) 119–133.
[48] J.-I. Yoshida, T. Maekawa, T. Murata, S.-I. Matsunaga, S. Isoe, J. Am. Chem. Soc. 112 (1990) 1962.